Artificial Intelligence in
Medical Imaging

Contents

Contents

ABOUT COVER

Editorial board member of *Artificial Intelligence in Medical Imaging*, Quan Zhou, MD, Professor, Department of Medical Imaging, The Third Affiliated Hospital of Southern Medical University, Guangzhou 510630, Guangdong Province, China

AIMS AND SCOPE

The primary aim of *Artificial Intelligence in Medical Imaging* (*AIMI, Artif Intell Med Imaging*) is to provide scholars and readers from various fields of artificial intelligence in medical imaging with a platform to publish high-quality basic and clinical research articles and communicate their research findings online.

    AIMI mainly publishes articles reporting research results obtained in the field of artificial intelligence in medical imaging and covering a wide range of topics, including artificial intelligence in radiology, pathology image analysis, endoscopy, molecular imaging, and ultrasonography.

INDEXING/ABSTRACTING

There is currently no indexing.

RESPONSIBLE EDITORS FOR THIS ISSUE

Production Editor: *Yan-Xia Xing*; **Production Department Director:** *Yu-Jie Ma*; **Editorial Office Director:** *Yun-Xiaojiao Wu*.

Artificial intelligence in coronary computed tomography angiography

Zhe-Zhe Zhang, Yan Guo, Yang Hou

ORCID number: Zhe-Zhe Zhang 0000-0002-4947-8270; Yan Guo 0000-0002-0565-640X; Yang Hou 0000-0002-9184-5441.

Zhe-Zhe Zhang, Yang Hou, Department of Radiology, Shengjing Hospital of China Medical University, Shenyang 110004, Liaoning Province, China

Yan Guo, GE Healthcare, Beijing 100176, China

Corresponding author: Yang Hou, PhD, Professor, Department of Radiology, Shengjing Hospital of China Medical University, No. 36 Sanhao Street, Heping District, Shenyang 110004, Liaoning Province, China. houyang1973@163.com

Abstract

Coronary computed tomography angiography (CCTA) is recommended as a frontline diagnostic tool in the non-invasive assessment of patients with suspected coronary artery disease (CAD) and cardiovascular risk stratification. To date, artificial intelligence (AI) techniques have brought major changes in the way that we make individualized decisions for patients with CAD. Applications of AI in CCTA have produced improvements in many aspects, including assessment of stenosis degree, determination of plaque type, identification of high-risk plaque, quantification of coronary artery calcium score, diagnosis of myocardial infarction, estimation of computed tomography-derived fractional flow reserve, left ventricular myocardium analysis, perivascular adipose tissue analysis, prognosis of CAD, and so on. The purpose of this review is to provide a comprehensive overview of current status of AI in CCTA.

Key Words: Coronary computed tomography angiography; Coronary artery disease; Artificial intelligence; Deep learning; Machine learning; Prognosis

Core Tip: The application of artificial intelligence in coronary computed tomography angiography mainly focuses on the following aspects: (1) Studies based on the coronary arteries and plaques for determination of stenosis degree, identification of plaque types, quantification of coronary artery calcium score, prediction of myocardial infarction, and prognosis evaluation; (2) Studies around the perivascular adipose tissue, which were mainly conducted using radiomics analysis and machine learning algorithm, for improvement of risk stratification; and (3) Studies based on the texture analysis of the left ventricular myocardium for assessment of functionally significant stenosis or for prognosis evaluation.

INTRODUCTION

Coronary computed tomography angiography (CCTA) has merged as a first-line diagnostic tool in the non-invasive evaluation of patients with suspected coronary artery disease (CAD), as recommended in the international guidelines[1,2]. With rich information provided in the luminal stenosis, the morphology and composition of plaques, and the overall circulation, CCTA can safely rule out the obstructive CAD and improve prognosis.

However, the information derived from CCTA images is recognized and interpreted by human readers, and varies among different scanning protocols, scanners, contrast medium injection protocols, and readers. The arrival of artificial intelligence (AI) brought hope that it can be applied for intelligent decision-making with autonomous acquired knowledge by identifying and extracting patterns among a group of observations[3,4].

With the frontline role of CCTA in the diagnostic strategies for CAD, "big data" is available and offers an optimal platform to bridge AI with CCTA. Recently, AI techniques in CCTA have gained much attention and have been widely applied in clinical care ranging from diagnosis to prognostic stratification. We seek to summarize the recent application of AI techniques in CCTA images, so as to investigate and identify the most important and promising research topics, the problems that have been resolved and remain to be resolved, and the future directions with many challenges and opportunities.

CURRENT APPLICATION OF AI IN CCTA

The application of AI in CCTA images mainly focuses on the following aspects: (1) Studies based on the coronary arteries and plaques for determination of stenosis degree, identification of plaque types, quantification of coronary artery calcium (CAC) score, prediction of myocardial infarction (MI), and prognosis evaluation; (2) studies around the perivascular adipose tissue (PVAT), which were mainly conducted using radiomics analysis and machine learning (ML) algorithm, for improvement of risk stratification; and (3) studies based on the texture analysis of the left ventricular myocardium (LVM) for assessment of functionally significant stenosis or for prognosis evaluation, as shown in Figure 1.

AUTOMATIC DETECTION AND CLASSIFICATION OF CORONARY ARTERY PLAQUE AND STENOSIS

Since different grades of coronary artery stenosis and varying types of plaque would lead to different patient management strategies, it is therefore crucial to: (1) Detect and determine the stenosis; (2) Detailedly characterize plaques (*i.e.,* non-calcified, calcified, mixed plaques); and (3) Identify the so-called "high-risk" plaque features. Recently, there are already applications of AI techniques in related CCTA fields, including stenosis evaluation and plaque characterization. Commonly, the anatomical evaluation of coronary stenosis and quantification of plaques rely on a relative accurate segmentation and successful automatic lesion localization in CCTA images. Several vendors are developing AI-based platform for stenosis evaluation. However, the identification of "high-risk" plaques remains challenging, and only a few studies have been proposed but are of great promise with prognostic value.

Kang *et al*[5] proposed a structured learning technique for automatic detection of obstructive and non-obstructive CAD on CCTA. Taking the visual identification of lesions with stenosis ≥ 25% by three expert readers, using consensus reading, as the reference standard, the method achieved a high sensitivity (93%), specificity (95%), and diagnostic accuracy (94%), with an area under the curve (AUC) of 0.94. Zreik *et al*
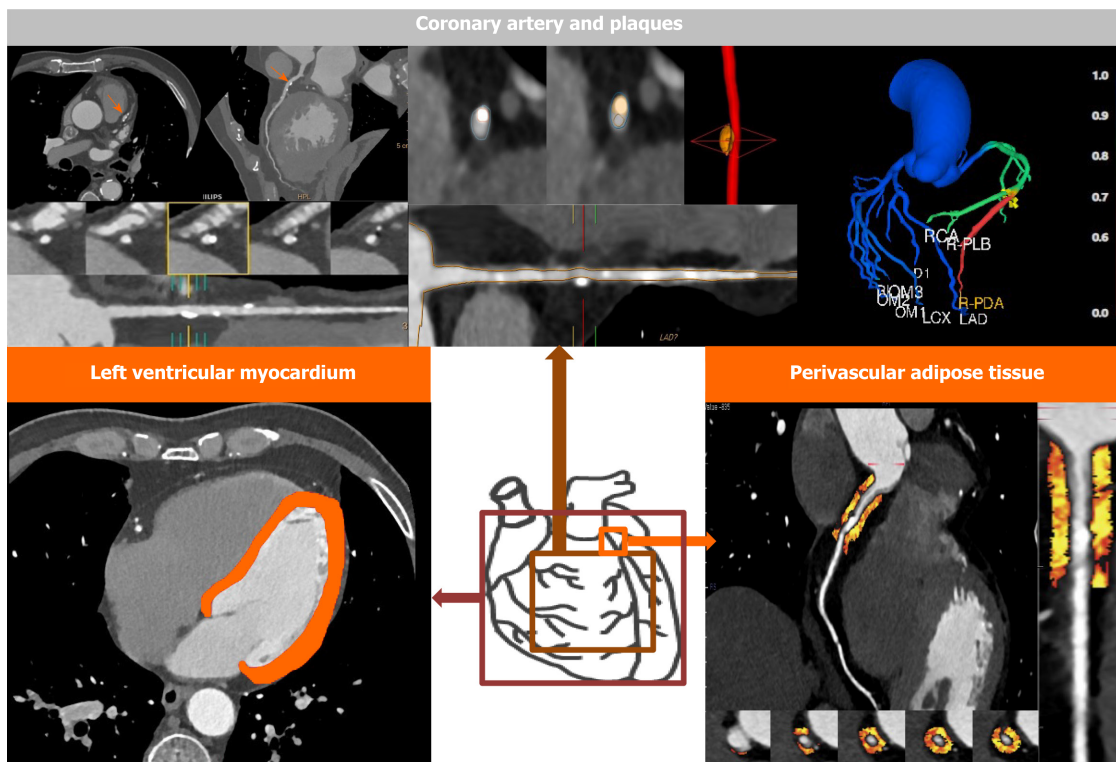
Figure 1 The application of artificial intelligence in coronary computed tomography angiography.

[6] employed a multi-task recurrent convolutional neural network to determine the stenosis severity based on the MPR view of a coronary artery extracted from the CCTA scan, as well as to automatically detect and characterize the coronary plaques. The approach achieved an accuracy of 0.80 for the determination of the anatomical significance of the coronary artery stenosis, and 0.77 for the detection and characterization of coronary plaques. Wei *et al*[7] developed a topological soft-gradient (TSG) detection method to prescreen for noncalcified plaque (NCP) candidates, which achieved AUCs of 0.87 ± 0.01 and 0.85 ± 0.01 in the training and validation sets, respectively. Jawaid *et al*[8] utilized support vector machine algorithms for automated detection of NCPs, and their approach achieved a detection accuracy of 88.4% with respect to the manual expert and a dice similarity coefficient of 83.2%.

In 2017, Kolossváry *et al*[9] investigated whether radiomics analysis improves the identification of coronary plaques with or without Napkin-ring sign (NRS). NRS is characterized as a so-called "high-risk" plaque features, which is defined as a plaque core with low CT attenuation apparently in contact with the lumen that is surrounded by a ring-shaped higher attenuation as napkin ring like in CCTA images[10,11]. However, the identification of the NRS remains challenging because it is assessed by a qualitative read of CCTA images which is affected by clinical experience and intra-/inter-reader variability[12]. Based on the segmented CCTA datasets, 8 conventional quantitative metrics and 4440 radiomic features were extracted. They found that none of the conventional quantitative parameters but 20.6% (916/4440) of radiomics features were significantly different between NRS and non-NRS plaques (Bonferroni-corrected $P < 0.0012$). In addition, almost half of the features (418/916) reached an AUC > 0.80, of which three features, including short- and long-run low gray-level emphasis and surface ratio of high attenuation voxels to total surface, exhibited excellent discriminatory value with AUCs of 0.918, 0.894, and 0.890, respectively. In 2019, the same research group validated the radiomics features extracted from CCTA in an *ex-vivo* histological study. One ML algorithm incorporating 13 parameters was superior compared with visual assessment (AUC = 0.73 *vs* 0.65) in the identification of advanced lesions[13].

DEEP LEARNING FOR AUTOMATIC CAC SCORING

CAC scoring plays a key role in risk stratification of CAD. Non-contrast-enhanced

cardiac CT, which is routinely acquired as a stand-alone test or an adjunct study prior to CCTA, is considered as the reference for quantification of CAC. CAC is defined as a high-attenuation area with > 130 HU in at least three contiguous pixels in non-contrast-enhanced cardiac CT. Recently, it has been shown that CAC can be also detected in CCTA images, which could reduce the radiation dose of a typical cardiac CT examination by 40%-50%[14]. Besides, the increased visibility of the coronary arteries in CCTA compared to non-contrast-enhanced cardiac CT could improve the identification of CAC. However, manual quantification of CAC requires substantial clinical experience to identify and make of every calcified lesion in each image slice, which is a time-consuming process. Consequently, a series of automatic methods have been proposed for CAC scoring in CCTA. Many investigations have shown promising results for clinical application in this field.

Some researchers[15,16] developed the automatic methods using two stages, including: (1) Segmentation of the coronary arteries; and (2) Identification of the CAC with the deviation from a trend line through the lumen intensity, or the voxels above a specific HU threshold, or the deviation from a model of non-calcified artery segments.

Wolterink *et al*[17,18] proposed an automatic CAC quantification method without a need for segmentation of the coronary artery tree in CCTA images using a combination of a convolutional neural network (CNN) and a Random Forest classifier. Thereafter, the same working group further extended and optimized their framework using a pair of CNNs in five ways[18], and the automatic CAC scoring in CCTA using a pair of CNNs yielded a high correlation (Pearson P = 0.950) and high consistency (intraclass correlation coefficient of 0.944) with the reference CAC scoring in non-contrast-enhanced CT.

In 2020, Fischer *et al*[19] proposed a novel fully automated algorithm using recurrent neural network with long short-term memory to detect CAC from CCTA data in a total of 565 vessels. An accuracy of 90.3% [95% confidence interval (CI): 88.0%-90.0%] was achieved on a per-vessel basis.

In summary, the CAC scoring performed on routine CCTA images without additional radiation exposure is highly desirable and the application of AI has provided considerable progress in the field and would become more influential in the clinical setting. In the near future, with the widespread application of AI techniques, CAC scoring using CCTA may eliminate the need for separate dedicated coronary calcium-scoring non-contrast enhanced CT scans.

IDENTIFICATION OF MYOCARDIAL ISCHEMIA

ML-based fractional flow reserve-CT for detection of functionally significant stenosis

It has been demonstrated that the anatomically significant appearance of a coronary stenosis is insufficient to detect hemodynamic significance and does not always equate with functional significance, which is particularly true for intermediate type coronary lesions[20,21]. Fractional flow reserve (FFR) performed during cardiac catheterization has been the reference standard in the detection of lesion-specific ischemia and is recommended for therapeutic decision-making[22]. However, the invasive measurement with a pressure wire and the relatively high cost restrict the clinical applica-tion of FFR.

Recently, novel non-invasive approaches utilizing ML algorithms for determination of FFR based on conventional CCTA images (FFR-CT) were developed and validated with a considerable diagnostic accuracy. The most popular algorithm is FFR-CT$_{ML}$ (Figure 2). FFR-CT$_{ML}$ was developed by Itu *et al*[23] in 2016 and provided by only one vendor (Siemens Healthineers, Germany) for research purpose. With the rapid development of AI, some FFR-CT platforms were provided for commercial use, such as the DEEPVESSE-FFR Platform provided by Keya Medical (Beijing, China). The DEEPVESSE-FFR Platform was developed by Wang *et al*[24] using MLNN + BRNN and has been commercially available since 2020.

So far, ML-based FFR-CT has been evaluated in several multi-center and single-center studies[23-35] using a threshold of ≤ 0.80 acquired from invasive FFR to detect lesion-specific ischemia. It has been demonstrated that ML-based FFR-CT performed equally in detecting flow-limiting stenosis compared with the computer fluid dynamics (CFD) based FFR-CT (FFR-CT$_{CFD}$)[26], while the FFR-CT$_{CFD}$ algorithm is time-consuming and heavily affected by the image quality[25,27,36]. The performance of ML-based FFR-CT in the related literature is summarized in Table 1.

Table 1 Summary of the current literature on machine learning-based fractional flow reserve-computed tomography

Ref.	Journal	Prospective	Multi- or single center	Platform	No. of patients	No. of vessels	Compared with CT-FFR$_{CFD}$	Accuracy	AUC
Itu *et al*[23], 2016	*Journal Application Physiology*	No	Single center	-	87	125	Yes	Per-lesion: 83%	Per-lesion: 0.90
Coenen *et al* [25], 2018	*Circulation: Cardiovascular Imaging*	Yes	The MACHINE registry	cFFR, version 2.1, Siemens	351	525	Yes	Per-lesion: 78%Per-patient: 85%	Per-lesion: 0.84
Tesche *et al* [26], 2018	*Radiology*	No	Single Center	cFFR, version 1.4, Siemens	85	104	Yes	Per-lesion: 88%; Per-patient: 92%	Per-lesion: 0.89; Per-patient: 0.91
Mastrodicasa *et al*[34], 2019	*Journal of Cardiovascular Computed Tomograph*	No	Single center	cFFR, version 3.0, Siemens	10/40	160	No	IRIS: 82%; FBP: 82%	-
Baumann *et al* [32], 2019	*European Journal of Radiology*	No	The MACHINE registry	cFFR, version 2.1, Siemens	351	525	No	-	Per-patient: Women:0.83; Men: 0.83
Doeberitz *et al* [27], 2019	*European Radiology*	No	Single center	cFFR, version 2.1, Siemens	48	103	No	-	Per-lesion: 0.93
Wang *et al* [24], 2019	*Journal of Geriatric Cardiology*	Yes	Single center	DEEPVESSE-FFR Platform	63	71	No	Per-lesion: 89%; Per-patient: 87%	Per-lesion: 0.93; Per-patient: 0.93
Tesche *et al* [30], 2020	*Journals of the American College of Cardiology: Cardiovascular Imaging*	Yes	The MACHINE registry	cFFR, version 2.1, Siemens	314	482	No	Per-lesion: 78%; CAC ≥ 400: 76%CAC 0-100: 79%; CAC 100-400: 76%	Total: 0.84 CAC ≥ 400: 0.71; CAC 0-400: 0.85
De Geer *et al* [31], 2019	*American Journal of Roentgenology*	No	The MACHINE registry	cFFR, version 2.1, Siemens	351	525	No	Total: 78%; 80 kv: 86%; 100 kv: 77%; 120 kv: 78%	Total: 0.84; 80 kv: 0.90; 100 kv: 0.82; 120 kv: 0.84
Xu *et al*[33], 2020	*European Radiology*	No	10 individual centers across China	cFFR, version 3.2.0, Siemens	437	570	No	Total: 89%; High quality: 94%; Low quality: 83%	Total: 0.89; High quality: 0.93; Low quality: 0.80
Kumamaru *et al*[28], 2020	*European Heart Journal - Cardiovascular Imaging*	No	Multi-center	Python 3.6	131	-	No	Per-patient: 76%	Per-patient: 0.78
Li *et al*[29], 2021	*Acta Radiologica*	No	Single center	DEEPVESSE-FFR Platform	73	85	No	Per-lesion: 92%; Per-patient: 91%	Per-lesion: 0.96
Xu *et al*[35], 2020	*European Radiology*	No	A Chinese multicenter study	cFFR, version 3.1.0, Siemens	442	544	No	Per lesion: 90%	-

IRIS: Iterative reconstruction in image space; FBP: Filtered back projection; CAC: Coronary artery calcium; FFR: Fractional flow reserve; AUC: Area under the curve; CT: Computed tomography.

In addition, the influences of CT reconstruction algorithms, image quality, tube voltage, coronary calcium, and gender on the diagnostic performance of FFR-CT$_{ML}$ were investigated in several studies. In a sub-study of MACHINE Registry, Tesche *et al* [30] examined the impact of calcification on CT-FFR$_{ML}$ determination and concluded that CT-FFR$_{ML}$ revealed a statistically significant different (P = 0.04) performance as Agatston calcium score increased: The AUC in high Agatston scores (CAC ≥ 400) was 0.71 (95%CI: 0.57-0.85) and in low-to-intermediate Agatston scores (CAC > 0 to < 400) was 0.85 (95%CI: 0.82-0.89). In another sub-study of MACHINE Registry, De Geer *et al* [31] examined the impact of different tube voltages on CT-FFRML determination and concluded that performance does not vary significantly between tube voltages of 100 kVp (AUC: 0.82) and 120 kVp (AUC: 0.84), while the AUC was 0.90 in examination with a tube voltage of 80 kVp. Based on data of the MACHINE Registry, Baumann *et al*
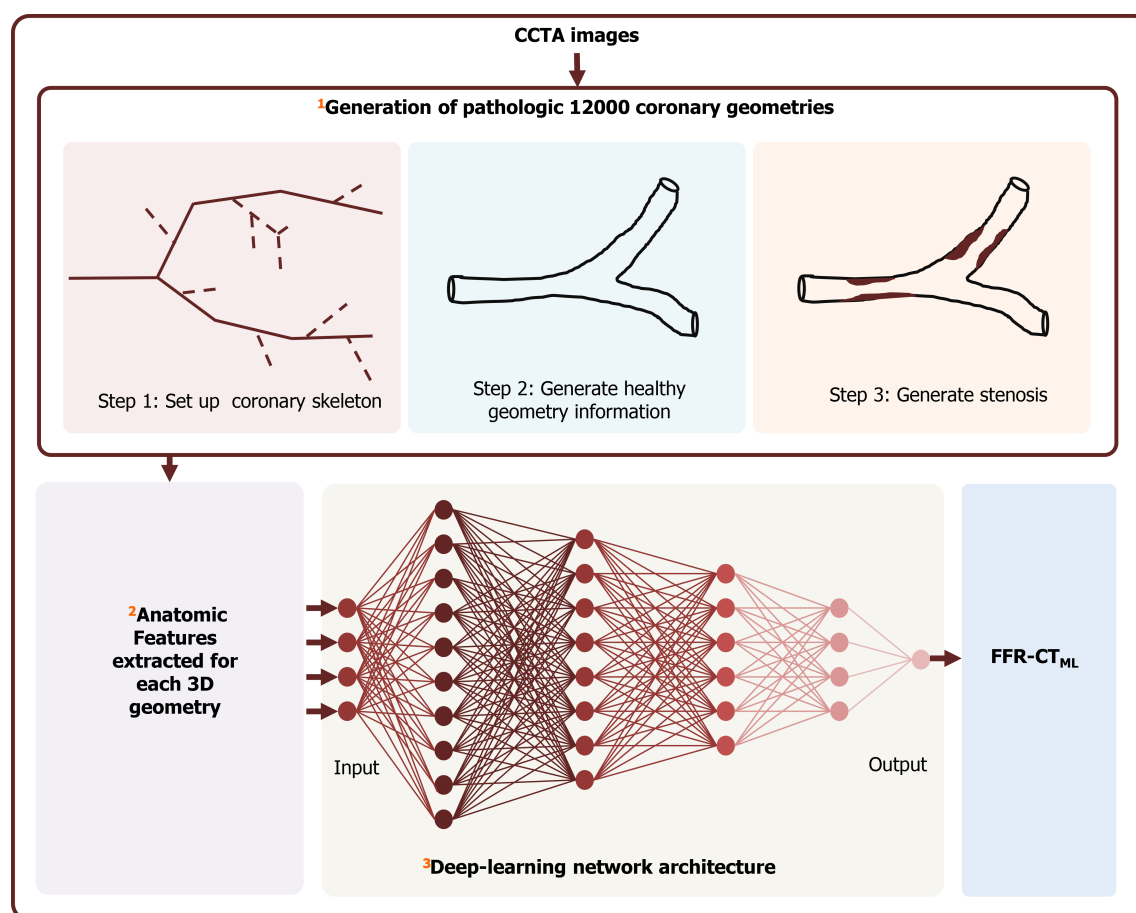
Figure 2 The workflow of the fractional flow reserve-computed tomography derivation. [1]A total of 12000 coronary anatomies were generated; [2]twenty-eight geometric features were extracted from the synthetically generated database; [3]a deep neural network with four hidden layers was used to train the machine learning-based model. FFR-CT: Fractional flow reserve-computed tomography; CCTA: Coronary computed tomography angiography.

[32] evaluated the impact of gender on the performance of FFRCTML and they found that FFRCTML performs equally in men and women (both with an AUC of 0.83). In a retrospective Chinese multicenter study, Xu *et al*[33] investigated the effect of image quality on the diagnostic performance of FFRCTML in 437 patients with 570 vessels. They found that the AUC of high-quality images [0.93 (95%CI: 0.88-0.98), *n* = 159] was significantly (*P* = 0.02) superior to that of low-quality images [0.80 (95%CI: 0.70-0.90), *n* = 92]. And CCTA with a score ≥ 3, intracoronary enhancement degree of 300–400 HU, and heart rate below 70 bpm at scanning could be of great benefit to more accurate FFRCTML analysis. In a retrospective single center study, Mastrodicasa *et al*[34] evaluated the influence of different CT reconstruction algorithms on the performance of CT-FFR$_{ML}$ in 40 CCTA datasets. CT-FFRML values were significantly different between iterative reconstruction in image space (IRIS) and filtered back projection algorithms, whereas no difference was observed in diagnostic accuracy (both 81.8%, *P* = 1.000). Additionally, they found that IRIS improved CT-FFRML post-processing speed significantly.

It should be mentioned that CT-FFR$_{ML}$ value for each location along the coronary is trained when taking the CT-FFR$_{CFD}$ as ground truth. Although the diagnostic accuracy of CT-FFR derived using deep learning (DL) methods was validated in several studies, it is still susceptible to the CCTA scanning factors. In the future, more attention should be paid to the widespread use of a local software solution that allows for image-variation and user-variation.

OTHER AI ALGORITHMS FOR PREDICTION OF MYOCARDIAL ISCHEMIA

Except for the ML based FFR-CT platforms described above, some other AI algorithms were developed recently for prediction of myocardial ischemia. These approaches are in early stage but show better interpretability, which were established *via* an

integration of qualitative or quantitative features derived from CCTA images and clinical factors.

In 2018, Dey *et al*[37] developed an integrated ML ischemia risk score (ML-IRS) from quantitative plaque measures using a supervised learning process to predict functionally significant stenosis in a prospective multicenter trial of 254 patients with 484 vessels. The ML-IRS exhibited a higher AUC (0.84) than conventional CCTA measures, including stenosis (0.76), LD-NCP volume (0.77), total plaque volume (0.74), and pre-test likelihood of CAD (0.63), for predicting lesion-specific ischemia by invasive FFR. Thereafter, the ML-IRS was integrated into coronary plaque analysis research software for generating a percent probability of pathological FFR on CCTA data.

In 2019, van Hamersvelt *et al*[38] proposed a DL method based on the LVM in resting CCTA images to identify functionally significant coronary artery stenosis using 126 patients. The DL approach achieved a higher AUC of 0.76 compared to degree of stenosis (AUC = 0.68).

In 2020, Shu *et al*[39] established a radiomics nomogram based on myocardial segments for predicting chronic myocardial ischemia using multivariate logistic regression. The accuracy of the nomogram for distinguishing chronic myocardial ischemia from normal myocardium was 0.839, 0.832, and 0.816 in the training, test, and validation cohorts, respectively.

PROGNOSTIC SIGNIFICANCE

PVAT-based radiomics for improving cardiac risk prediction

Early detection of vascular inflammation, which is a major contributor to athero-genesis and atherosclerotic plaque rupture[40,41], would enable better cardiovascular risk stratification[42]. The vascular inflammation can be detected by characterizing the phenotypic changes in PVAT using the fat attenuation index (FAI) in routine CCTA images[43,44]. FAI was defined as the average attenuation of all voxels with attenuation values between -190 HU and -30 HU located within a radial distance from the outer coronary artery wall equal to the average diameter of the respective vessel, as described previously[43,44]. However, FAI is an average of the voxel intensity values and does not account for the complex spatial relationship among voxels.

Recently, some studies investigated whether radiomics analysis could help to extract more information from the PVAT that cannot be captured by human eyes. The radiomics features surrounding PVAT mainly include two parts: (1) PVAT surrounding the standardized coronary segments, which was often investigated at a per-patient level; and (2) PVAT around the target lesion, which was at a per-lesion level.

As for the per-patient level, Oikonomou *et al*[45] developed an AI-powered radiotranscriptomic signature for predicting cardiac risk based on the radiomics features extracted from PVAT around the proximal to distal right coronary artery (RCA) and the left coronary artery in CCTA images. A fat radiomic profile (FRP) was established, using random forest model based on the features extracted from the standardized coronary segments, to distinguish the 101 patients who experienced major adverse cardiac events (MACE) within 5 years from 101 matched controls. The FRP was significantly associated with the risk of MACE [adjusted hazard ratio (HR): 1.12, 95%CI: 1.08-1.15, $P < 0.001$]. And patients with an FRP ≥ 0.63 had a 10.8-fold higher risk of MACE than those with an FRP < 0.63, after adjusted for clinical factors. The AUC of FRP in predicting MACE was 0.774 (95%CI: 0.622-0.926) in the external validation dataset (20% of the 202 samples). When added to the traditional model, FRP improved the distinguishing performance from an AUC of 0.754 to 0.880. Additionally, they found that FRP was significantly higher in 44 patients with acute MI compared with 44 controls ($P < 0.001$), but unlike FAI, FRP remained unchanged 6 mo later in 16 patients with acute MI (AMI), confirming that FRP detects persistent PVAT changes that cannot be captured by FAI.

As for the per-lesion level, in 2020, Lin *et al*[46] further explored the prognostic value of the radiomics features of PVAT around not only the standardized coronary segments but also lesions in a prospective case-control study. They found no significant difference between the PVAT radiomics features of culprit and non-culprit lesions in patients with AMI, lending further support to the pan-coronary inflam-matory hypothesis. But on the other hand, as for the per-patient level, patients with AMI ($n = 60$) have a distinct PVAT radiomics phenotype surrounding the proximal RCA compared with patients with stable (matched, $n = 60$) or no CAD (matched, $n = $

60). Among the three models that they developed, the PVAT-based radiomics model (AUC: 0.87) outperforms the clinical model (AUC: 0.76) and the combined model incorporating clinical factors and PVAT attenuation (AUC: 0.77) in identifying AMI with stable CAD and controls. Additionally, after a 6-mo follow-up of patients with AMI, no significant change was observed in the radiomics features of PVAT surrounding the proximal RCA or non-culprit lesions.

QUANTITATIVE CT FEATURES-BASED ML FOR OUTCOME PREDICTION

Information extracted from CCTA images along with other clinical factors are associated with prognosis, and AI technology demonstrated great potential to enhance decision-making and improve patient outcomes. Currently, the prognostic value of ML algorithms using quantitative CCTA features together with clinical variables was investigated by researchers in several studies[47-53], in which promising results were obtained. The ML algorithms performed better than traditional predictors, not only for short-term treatment decisions but also for long-term risk predictions, as summarized in Table 2.

One of the first major studies using CCTA based ML approach for prognosis evaluation is a large prospective multi-center study conducted by Motwani *et al*[48] in 2017. They developed an ML model in CCTA to predict 5-year all-cause mortality using a dataset of 10030 patients with suspected CAD from the CONFIRM registry (Coronary CT Angiography Evaluation for Clinical Outcomes: An International Multicenter). The ML model was established after an automated feature selection procedure based on 44 CCTA-derived parameters and 25 clinical parameters. One summary score for clinical parameters (Framingham risk score, FRS) and three composite CCTA-based scores [including the segment stenosis score (SSS), the segment involvement score (SIS), and the modified Duke prognostic CAD index (DI)] were derived. The ML model exhibited a significant higher AUC compared with the conventional scores alone for predicting 5-year all-cause mortality (ML: 0.79 *vs* FRS: 0.61, SSS: 0.64, SIS: 0.64, and DI: 0.62; $P < 0.001$).

Two years later, in 2019, Johnson *et al*[49] developed another ML model using 64 vessel features derived from CCTA images, to discriminate between patients with and without subsequent death or cardiovascular events in a retrospective single-center study with 6892 patients. The performance of the ML model was compared with that of Coronary Artery Disease Reporting and Data System (CAD-RADS) score. For prediction of all-cause mortality, the AUC of the ML model was significantly higher than that of CAD-RADS (0.77 *vs* 0.72, $P < 0.001$). For prediction of coronary artery deaths, the AUC was significantly higher for the ML model than for CAD-RADS (0.85 *vs* 0.79, $P < 0.001$).

In 2020, Commandeur *et al*[52] developed an ML model integrating clinical parameters with quantitative imaging-based variables for predicting events of long-term risk of MI and cardiac death in asymptomatic subjects using the dataset with 1912 cases from the randomized EISNER trial. The ML model obtained a significantly higher AUC than atherosclerotic cardiovascular disease (ASCVD) risk and CAC score for predicting events (ML: 0.82; ASCVD: 0.77; CAC: 0.77; $P < 0.05$). Subjects with a higher ML score had a significant high hazard of suffering events (HR: 10.38, $P < 0.001$).

As for the short-term decision-making, in 2020, Kwan *et al*[53] examined whether the ML-IRS, developed by Dey *et al*[37] in 2018, as described previously (Figures 1 and 2), can predict revascularization in patients referred to ICA after CCTA in a prospective dual-center study of 352 patients with 1056 analyzable vessels. It would be beneficial to effectively identify the patients who were referred for standard clinical CCTA followed by ICA due to decision by a primary treating physician but did not receive revascularization, because those patients are a high-cost population with low yield from the invasive procedure. The results indicated that ML-IRS, when added to the traditional risk model, significantly improve the prediction of future revascularization with an increased AUC from 0.69 (95%CI: 0.65-0.72) to 0.78 (95%CI: 0.75-0.81) ($P < 0.0001$).

Overall, the application of AI in CCTA has a potential future for improving the short-term risk stratification and long-term prognostic evaluation. The ML algorithms that have been proposed should be validated and tested in real world with larger external cohorts including diversity of patients so as to make sure the models be optimized and generalized.

Table 2 summary of the current literature on the prognostic value of machine learning algorithms in coronary computed tomography angiography

Ref.	Journal	Prospective	Multi Center	No. of Patients	No. of Events	Algorithm	Endpoint	Follow-up time	Performance
Motwani *et al* [48], 2017	*European Heart Journal*	Yes	Yes	10030	745 died	LogitBoost	5-yr all-cause mortality	5.4 ± 1.4 yr	AUC = 0.79
van Rosendael *et al*[47], 2018	*Journal of Cardiovascular Computed Tomograph*	Yes	Yes	8844	350 death and 259 non-fatal MI	XGBoost	MI and death	4.6 ± 1.5 yr	AUC = 0.77
Johnson *et al* [49], 2019	*Radiology*	No	No	6892	380 died of all causes and 70 died of CAD	Logistic regression, KNN, Bagged trees, and classification neural network	Death or cardiovascular events	9.0 yr (interquartile range, 8.2–9.8 yr)	For all-cause mortality: AUC = 0.77; For CAD deaths: AUC = 0.85
van Assen *et al* [50], 2019	*European Journal of Radiology*	No	No	45	16 MACEs	Regression analysis	MACE	12 mo	AUC = 0.94
von Knebel Doeberitz *et al* [51], 2019	*The American Journal of Cardiology*	No	No	82	18 MACEs	Integration of CT-FFR, stenosis ≥ 50% and plaque markers	MACE	18.5 mo (interquartile range 11.5 to 26.6 mo)	AUC = 0.94
Commandeur *et al*[52], 2020	*Cardiovascular Research*	Yes		1912	76 MI and/or cardiac death	ML	Long-term risk of MI and cardiac death	14.5 ± 2 yr	AUC = 0.82
Kwan *et al* [53], 2021	*European Radiology*	Yes	Yes	352		ML	Future revascularization		AUC = 0.78

XGBoost: Extreme gradient boosting; KNN: K-nearest neighbors; ML: Machine learning; AUC: Area under the curve; MACE: Major adverse cardiac events; CT-FFR: Computed tomography-fractional flow reserve; CAD: Coronary artery disease; MI: Myocardial infarction.

CONCLUSION

Current AI applications in CCTA images are mostly designed in two dimensions: (1) For the radiologists, AI is applied to improve efficiency and reduce workload *via* optimizing the clinical workflow, such as improvement of image reconstruction from lower quality to high quality (*e.g.*, low-dose acquisition or motion artifacts) and structured reporting; and (2) For the patients, AI is utilized to increase benefit and improve prognostic evaluation *via* providing valuable diagnostic information more accurately, such as detection of anatomic and functional stenosis, quantification of plaques, and estimation of the vascular inflammation.

In this review, we mainly focused on the second dimension which is patient oriented. AI algorithms in CCTA images provide information in a more objective, reproducible, and rational manner compared to human perception, and exhibits its potential to outperform human in several cardiac fields. However, CCTA imaging lagged behind cancer imaging in the clinical translational of AI-based methods, especially the radiomics analysis. It has long been demonstrated in the field of cancer imaging that radiomics signatures are superior to traditional factors in predicting outcomes of patients. But only a few studies using radiomics analysis have been conducted in CCTA images. Considering that regions of interest (ROIs) segmented before the extraction of radiomics features, can be drawn along the edge of the tumor in cancer imaging generally, in CCTA images the selection of ROIs brings about challenges. Researchers hereby performed radiomics analysis around the PVAT or LVM or plaques. And recently, several groups succeeded in developing automated segmentation of PVAT and LVM, which provides probabilities to explore more novel non-invasive predictors for improvement of risk stratification and prognosis in patients with CAD.

Additionally, FFR-CT driven by AI is a hot topic in recent years. Various FFR-CT platforms are developed and adding into the clinical diagnostic workflow for not only research purpose but also commercial use. In the near future, the FFR-CT platforms

would bring major changes in the way to make decisions for patients with CAD before invasive coronary angiography.

However, before AI solutions can be truly widely implemented in daily clinical workflow or the reading room, several issues should be noted: (1) The algorithms need to be carefully validated in multi-center studies or large clinical trials to ensure the robustness and generalization; (2) The approval of clinical application is required to prove the accuracy and safety of the AI products; and (3) The legal and ethical issues should be taken into consideration.

In summary, AI offers the possibility to optimize clinical workflow and provide precise information for diagnostic and treatment, which will benefit both radiologists and patients. However, it is pertinent to note that AI will not simply substitute the cardiac radiologists, and human support or supervision is still needed. Rather, the cardiac radiologists need to be fully aware of the strengths and limitations of AI.

ACKNOWLEDGEMENTS

REFERENCES

1   **Padley SPG**, Roditi G, Nicol ED; BSCI/BSCCT. Chest pain of recent onset: assessment and diagnosis (CG95). A step change in the requirement for cardiovascular CT. *Clin Radiol* 2017; **72**: 751-753 [PMID: 28647044 DOI: 10.1016/j.crad.2017.04.020]

2   **Knuuti J**, Wijns W, Saraste A, Capodanno D, Barbato E, Funck-Brentano C, Prescott E, Storey RF, Deaton C, Cuisset T, Agewall S, Dickstein K, Edvardsen T, Escaned J, Gersh BJ, Svitil P, Gilard M, Hasdai D, Hatala R, Mahfoud F, Masip J, Muneretto C, Valgimigli M, Achenbach S, Bax JJ; ESC Scientific Document Group. 2019 ESC Guidelines for the diagnosis and management of chronic coronary syndromes. *Eur Heart J* 2020; **41**: 407-477 [PMID: 31504439 DOI: 10.1093/eurheartj/ehz425]

3   **Lamata P**. Teaching cardiovascular medicine to machines. *Cardiovasc Res* 2018; **114**: e62-e64 [PMID: 29850780 DOI: 10.1093/cvr/cvy127]

4   **Deo RC**. Machine Learning in Medicine. *Circulation* 2015; **132**: 1920-1930 [PMID: 26572668 DOI: 10.1161/CIRCULATIONAHA.115.001593]

5   **Kang D**, Dey D, Slomka PJ, Arsanjani R, Nakazato R, Ko H, Berman DS, Li D, Kuo CC. Structured learning algorithm for detection of nonobstructive and obstructive coronary plaque lesions from computed tomography angiography. *J Med Imaging (Bellingham)* 2015; **2**: 014003 [PMID: 26158081 DOI: 10.1117/1.JMI.2.1.014003]

6   **Zreik M**, van Hamersvelt RW, Wolterink JM, Leiner T, Viergever MA, Isgum I. A Recurrent CNN for Automatic Detection and Classification of Coronary Artery Plaque and Stenosis in Coronary CT Angiography. *IEEE Trans Med Imaging* 2019; **38**: 1588-1598 [PMID: 30507498 DOI: 10.1109/TMI.2018.2883807]

7   **Wei J**, Zhou C, Chan HP, Chughtai A, Agarwal P, Kuriakose J, Hadjiiski L, Patel S, Kazerooni E. Computerized detection of noncalcified plaques in coronary CT angiography: evaluation of topological soft gradient prescreening method and luminal analysis. *Med Phys* 2014; **41**: 081901 [PMID: 25086532 DOI: 10.1118/1.4885958]

8   **Jawaid MM**, Riaz A, Rajani R, Reyes-Aldasoro CC, Slabaugh G. Framework for detection and localization of coronary non-calcified plaques in cardiac CTA using mean radial profiles. *Comput Biol Med* 2017; **89**: 84-95 [PMID: 28797740 DOI: 10.1016/j.compbiomed.2017.07.021]

9   **Kolossváry M**, Kárády J, Szilveszter B, Kitslaar P, Hoffmann U, Merkely B, Maurovich-Horvat P. Radiomic Features Are Superior to Conventional Quantitative Computed Tomographic Metrics to Identify Coronary Plaques With Napkin-Ring Sign. *Circ Cardiovasc Imaging* 2017; **10**: e006843 [PMID: 29233836 DOI: 10.1161/CIRCIMAGING.117.006843]

10   **Narula J**, Achenbach S. Napkin-ring necrotic cores: defining circumferential extent of necrotic cores in unstable plaques. *JACC Cardiovasc Imaging* 2009; **2**: 1436-1438 [PMID: 20083080 DOI: 10.1016/j.jcmg.2009.10.004]

11   **Maurovich-Horvat P**, Hoffmann U, Vorpahl M, Nakano M, Virmani R, Alkadhi H. The napkin-ring sign: CT signature of high-risk coronary plaques? *JACC Cardiovasc Imaging* 2010; **3**: 440-444 [PMID: 20394906 DOI: 10.1016/j.jcmg.2010.02.003]

12   **Puchner SB**, Liu T, Mayrhofer T, Truong QA, Lee H, Fleg JL, Nagurney JT, Udelson JE, Hoffmann U, Ferencik M. High-risk plaque detected on coronary CT angiography predicts acute coronary syndromes independent of significant stenosis in acute chest pain: results from the ROMICAT-II trial.

J Am Coll Cardiol 2014; **64**: 684-692 [PMID: 25125300 DOI: 10.1016/j.jacc.2014.05.039]

13   **Kolossváry M**, Karády J, Kikuchi Y, Ivanov A, Schlett CL, Lu MT, Foldyna B, Merkely B, Aerts HJ, Hoffmann U, Maurovich-Horvat P. Radiomics versus Visual and Histogram-based Assessment to Identify Atheromatous Lesions at Coronary CT Angiography: An ex Vivo Study. *Radiology* 2019; **293**: 89-96 [PMID: 31385755 DOI: 10.1148/radiol.2019190407]

14   **Voros S**, Qian Z. Agatston score tried and true: by contrast, can we quantify calcium on CTA? *J Cardiovasc Comput Tomogr* 2012; **6**: 45-47 [PMID: 22264631 DOI: 10.1016/j.jcct.2011.12.002]

15   **Ahmed W**, de Graaf MA, Broersen A, Kitslaar PH, Oost E, Dijkstra J, Bax JJ, Reiber JH, Scholte AJ. Automatic detection and quantification of the Agatston coronary artery calcium score on contrast computed tomography angiography. *Int J Cardiovasc Imaging* 2015; **31**: 151-161 [PMID: 25159031 DOI: 10.1007/s10554-014-0519-4]

16   **Eilot D**, Goldenberg R. Fully automatic model-based calcium segmentation and scoring in coronary CT angiography. *Int J Comput Assist Radiol Surg* 2014; **9**: 595-608 [PMID: 24203575 DOI: 10.1007/s11548-013-0955-y]

17   **Wolterink JM**, Leiner T, de Vos BD, Coatrieux JL, Kelm BM, Kondo S, Salgado RA, Shahzad R, Shu H, Snoeren M, Takx RA, van Vliet LJ, van Walsum T, Willems TP, Yang G, Zheng Y, Viergever MA, Išgum I. An evaluation of automatic coronary artery calcium scoring methods with cardiac CT using the orCaScore framework. *Med Phys* 2016; **43**: 2361 [PMID: 27147348 DOI: 10.1118/1.4945696]

18   **Wolterink JM**, Leiner T, de Vos BD, van Hamersvelt RW, Viergever MA, Išgum I. Automatic coronary artery calcium scoring in cardiac CT angiography using paired convolutional neural networks. *Med Image Anal* 2016; **34**: 123-136 [PMID: 27138584 DOI: 10.1016/j.media.2016.04.004]

19   **Fischer AM**, Eid M, De Cecco CN, Gulsun MA, van Assen M, Nance JW, Sahbaee P, De Santis D, Bauer MJ, Jacobs BE, Varga-Szemes A, Kabakus IM, Sharma P, Jackson LJ, Schoepf UJ. Accuracy of an Artificial Intelligence Deep Learning Algorithm Implementing a Recurrent Neural Network With Long Short-term Memory for the Automated Detection of Calcified Plaques From Coronary Computed Tomography Angiography. *J Thorac Imaging* 2020; **35** Suppl 1: S49-S57 [PMID: 32168163 DOI: 10.1097/RTI.0000000000000491]

20   **Meijboom WB**, Van Mieghem CA, van Pelt N, Weustink A, Pugliese F, Mollet NR, Boersma E, Regar E, van Geuns RJ, de Jaegere PJ, Serruys PW, Krestin GP, de Feyter PJ. Comprehensive assessment of coronary artery stenoses: computed tomography coronary angiography versus conventional coronary angiography and correlation with fractional flow reserve in patients with stable angina. *J Am Coll Cardiol* 2008; **52**: 636-643 [PMID: 18702967 DOI: 10.1016/j.jacc.2008.05.024]

21   **Conte E**, Sonck J, Mushtaq S, Collet C, Mizukami T, Barbato E, Tanzilli A, Nicoli F, De Bruyne B, Andreini D. FFR$_{CT}$ and CT perfusion: A review on the evaluation of functional impact of coronary artery stenosis by cardiac CT. *Int J Cardiol* 2020; **300**: 289-296 [PMID: 31466886 DOI: 10.1016/j.ijcard.2019.08.018]

22   **Tonino PA**, De Bruyne B, Pijls NH, Siebert U, Ikeno F, van' t Veer M, Klauss V, Manoharan G, Engstrøm T, Oldroyd KG, Ver Lee PN, MacCarthy PA, Fearon WF; FAME Study Investigators. Fractional flow reserve versus angiography for guiding percutaneous coronary intervention. *N Engl J Med* 2009; **360**: 213-224 [PMID: 19144937 DOI: 10.1056/NEJMoa0807611]

23   **Itu L**, Rapaka S, Passerini T, Georgescu B, Schwemmer C, Schoebinger M, Flohr T, Sharma P, Comaniciu D. A machine-learning approach for computation of fractional flow reserve from coronary computed tomography. *J Appl Physiol (1985)* 2016; **121**: 42-52 [PMID: 27079692 DOI: 10.1152/japplphysiol.00752.2015]

24   **Wang ZQ**, Zhou YJ, Zhao YX, Shi DM, Liu YY, Liu W, Liu XL, Li YP. Diagnostic accuracy of a deep learning approach to calculate FFR from coronary CT angiography. *J Geriatr Cardiol* 2019; **16**: 42-48 [PMID: 30800150 DOI: 10.11909/j.issn.1671-5411.2019.01.010]

25   **Coenen A**, Kim YH, Kruk M, Tesche C, De Geer J, Kurata A, Lubbers ML, Daemen J, Itu L, Rapaka S, Sharma P, Schwemmer C, Persson A, Schoepf UJ, Kepka C, Hyun Yang D, Nieman K. Diagnostic Accuracy of a Machine-Learning Approach to Coronary Computed Tomographic Angiography-Based Fractional Flow Reserve: Result From the MACHINE Consortium. *Circ Cardiovasc Imaging* 2018; **11**: e007217 [PMID: 29914866 DOI: 10.1161/CIRCIMAGING.117.007217]

26   **Tesche C**, De Cecco CN, Baumann S, Renker M, McLaurin TW, Duguay TM, Bayer RR 2nd, Steinberg DH, Grant KL, Canstein C, Schwemmer C, Schoebinger M, Itu LM, Rapaka S, Sharma P, Schoepf UJ. Coronary CT Angiography-derived Fractional Flow Reserve: Machine Learning Algorithm versus Computational Fluid Dynamics Modeling. *Radiology* 2018; **288**: 64-72 [PMID: 29634438 DOI: 10.1148/radiol.2018171291]

27   **von Knebel Doeberitz PL**, De Cecco CN, Schoepf UJ, Duguay TM, Albrecht MH, van Assen M, Bauer MJ, Savage RH, Pannell JT, De Santis D, Johnson AA, Varga-Szemes A, Bayer RR, Schönberg SO, Nance JW, Tesche C. Coronary CT angiography-derived plaque quantification with artificial intelligence CT fractional flow reserve for the identification of lesion-specific ischemia. *Eur Radiol* 2019; **29**: 2378-2387 [PMID: 30523456 DOI: 10.1007/s00330-018-5834-z]

28   **Kumamaru KK**, Fujimoto S, Otsuka Y, Kawasaki T, Kawaguchi Y, Kato E, Takamura K, Aoshima C, Kamo Y, Kogure Y, Inage H, Daida H, Aoki S. Diagnostic accuracy of 3D deep-learning-based fully automated estimation of patient-level minimum fractional flow reserve from coronary computed tomography angiography. *Eur Heart J Cardiovasc Imaging* 2020; **21**: 437-445 [PMID: 31230076 DOI: 10.1093/ehjci/jez160]

29   **Li Y**, Qiu H, Hou Z, Zheng J, Li J, Yin Y, Gao R. Additional value of deep learning computed

tomographic angiography-based fractional flow reserve in detecting coronary stenosis and predicting outcomes. *Acta Radiol* 2021; 284185120983977 [PMID: 33423530 DOI: 10.1177/0284185120983977]

30   **Tesche C**, Otani K, De Cecco CN, Coenen A, De Geer J, Kruk M, Kim YH, Albrecht MH, Baumann S, Renker M, Bayer RR, Duguay TM, Litwin SE, Varga-Szemes A, Steinberg DH, Yang DH, Kepka C, Persson A, Nieman K, Schoepf UJ. Influence of Coronary Calcium on Diagnostic Performance of Machine Learning CT-FFR: Results From MACHINE Registry. *JACC Cardiovasc Imaging* 2020; **13**: 760-770 [PMID: 31422141 DOI: 10.1016/j.jcmg.2019.06.027]

31   **De Geer J**, Coenen A, Kim YH, Kruk M, Tesche C, Schoepf UJ, Kepka C, Yang DH, Nieman K, Persson A. Effect of Tube Voltage on Diagnostic Performance of Fractional Flow Reserve Derived From Coronary CT Angiography With Machine Learning: Results From the MACHINE Registry. *AJR Am J Roentgenol* 2019; **213**: 325-331 [PMID: 31039021 DOI: 10.2214/AJR.18.20774]

32   **Baumann S**, Renker M, Schoepf UJ, De Cecco CN, Coenen A, De Geer J, Kruk M, Kim YH, Albrecht MH, Duguay TM, Jacobs BE, Bayer RR, Litwin SE, Weiss C, Akin I, Borggrefe M, Yang DH, Kepka C, Persson A, Nieman K, Tesche C. Gender differences in the diagnostic performance of machine learning coronary CT angiography-derived fractional flow reserve -results from the MACHINE registry. *Eur J Radiol* 2019; **119**: 108657 [PMID: 31521876 DOI: 10.1016/j.ejrad.2019.108657]

33   **Xu PP**, Li JH, Zhou F, Jiang MD, Zhou CS, Lu MJ, Tang CX, Zhang XL, Yang L, Zhang YX, Wang YN, Zhang JY, Yu MM, Hou Y, Zheng MW, Zhang B, Zhang DM, Yi Y, Xu L, Hu XH, Liu H, Lu GM, Ni QQ, Zhang LJ. The influence of image quality on diagnostic performance of a machine learning-based fractional flow reserve derived from coronary CT angiography. *Eur Radiol* 2020; **30**: 2525-2534 [PMID: 32006167 DOI: 10.1007/s00330-019-06571-4]

34   **Mastrodicasa D**, Albrecht MH, Schoepf UJ, Varga-Szemes A, Jacobs BE, Gassenmaier S, De Santis D, Eid MH, van Assen M, Tesche C, Mantini C, De Cecco CN. Artificial intelligence machine learning-based coronary CT fractional flow reserve (CT-FFR$_{ML}$): Impact of iterative and filtered back projection reconstruction techniques. *J Cardiovasc Comput Tomogr* 2019; **13**: 331-335 [PMID: 30391256 DOI: 10.1016/j.jcct.2018.10.026]

35   **Di Jiang M**, Zhang XL, Liu H, Tang CX, Li JH, Wang YN, Xu PP, Zhou CS, Zhou F, Lu MJ, Zhang JY, Yu MM, Hou Y, Zheng MW, Zhang B, Zhang DM, Yi Y, Xu L, Hu XH, Yang J, Lu GM, Ni QQ, Zhang LJ. The effect of coronary calcification on diagnostic performance of machine learning-based CT-FFR: a Chinese multicenter study. *Eur Radiol* 2021; **31**: 1482-1493 [PMID: 32929641 DOI: 10.1007/s00330-020-07261-2]

36   **Gaur S**, Øvrehus KA, Dey D, Leipsic J, Bøtker HE, Jensen JM, Narula J, Ahmadi A, Achenbach S, Ko BS, Christiansen EH, Kaltoft AK, Berman DS, Bezerra H, Lassen JF, Nørgaard BL. Coronary plaque quantification and fractional flow reserve by coronary computed tomography angiography identify ischaemia-causing lesions. *Eur Heart J* 2016; **37**: 1220-1227 [PMID: 26763790 DOI: 10.1093/eurheartj/ehv690]

37   **Dey D**, Gaur S, Ovrehus KA, Slomka PJ, Betancur J, Goeller M, Hell MM, Gransar H, Berman DS, Achenbach S, Botker HE, Jensen JM, Lassen JF, Norgaard BL. Integrated prediction of lesion-specific ischaemia from quantitative coronary CT angiography using machine learning: a multicentre study. *Eur Radiol* 2018; **28**: 2655-2664 [PMID: 29352380 DOI: 10.1007/s00330-017-5223-z]

38   **van Hamersvelt RW**, Zreik M, Voskuil M, Viergever MA, Išgum I, Leiner T. Deep learning analysis of left ventricular myocardium in CT angiographic intermediate-degree coronary stenosis improves the diagnostic accuracy for identification of functionally significant stenosis. *Eur Radiol* 2019; **29**: 2350-2359 [PMID: 30421020 DOI: 10.1007/s00330-018-5822-3]

39   **Shu ZY**, Cui SJ, Zhang YQ, Xu YY, Hung SC, Fu LP, Pang PP, Gong XY, Jin QY. Predicting Chronic Myocardial Ischemia Using CCTA-Based Radiomics Machine Learning Nomogram. *J Nucl Cardiol* 2020 epub ahead of print [PMID: 32557238 DOI: 10.1007/s12350-020-02204-2]

40   **Ridker PM**, Everett BM, Thuren T, MacFadyen JG, Chang WH, Ballantyne C, Fonseca F, Nicolau J, Koenig W, Anker SD, Kastelein JJP, Cornel JH, Pais P, Pella D, Genest J, Cifkova R, Lorenzatti A, Forster T, Kobalava Z, Vida-Simiti L, Flather M, Shimokawa H, Ogawa H, Dellborg M, Rossi PRF, Troquay RPT, Libby P, Glynn RJ; CANTOS Trial Group. Antiinflammatory Therapy with Canakinumab for Atherosclerotic Disease. *N Engl J Med* 2017; **377**: 1119-1131 [PMID: 28845751 DOI: 10.1056/NEJMoa1707914]

41   **Ridker PM**, Libby P, MacFadyen JG, Thuren T, Ballantyne C, Fonseca F, Koenig W, Shimokawa H, Everett BM, Glynn RJ. Modulation of the interleukin-6 signalling pathway and incidence rates of atherosclerotic events and all-cause mortality: analyses from the Canakinumab Anti-Inflammatory Thrombosis Outcomes Study (CANTOS). *Eur Heart J* 2018; **39**: 3499-3507 [PMID: 30165610 DOI: 10.1093/eurheartj/ehy310]

42   **Ross R**. Atherosclerosis--an inflammatory disease. *N Engl J Med* 1999; **340**: 115-126 [PMID: 9887164 DOI: 10.1056/NEJM199901143400207]

43   **Antonopoulos AS**, Sanna F, Sabharwal N, Thomas S, Oikonomou EK, Herdman L, Margaritis M, Shirodaria C, Kampoli AM, Akoumianakis I, Petrou M, Sayeed R, Krasopoulos G, Psarros C, Ciccone P, Brophy CM, Digby J, Kelion A, Uberoi R, Anthony S, Alexopoulos N, Tousoulis D, Achenbach S, Neubauer S, Channon KM, Antoniades C. Detecting human coronary inflammation by imaging perivascular fat. *Sci Transl Med* 2017; **9**: eaal2658 [PMID: 28701474 DOI: 10.1126/scitranslmed.aal2658]

44   **Oikonomou EK**, Marwan M, Desai MY, Mancio J, Alashi A, Hutt Centeno E, Thomas S, Herdman

L, Kotanidis CP, Thomas KE, Griffin BP, Flamm SD, Antonopoulos AS, Shirodaria C, Sabharwal N, Deanfield J, Neubauer S, Hopewell JC, Channon KM, Achenbach S, Antoniades C. Non-invasive detection of coronary inflammation using computed tomography and prediction of residual cardiovascular risk (the CRISP CT study): a post-hoc analysis of prospective outcome data. *Lancet* 2018; **392**: 929-939 [PMID: 30170852 DOI: 10.1016/S0140-6736(18)31114-0]

45   **Oikonomou EK**, Williams MC, Kotanidis CP, Desai MY, Marwan M, Antonopoulos AS, Thomas KE, Thomas S, Akoumianakis I, Fan LM, Kesavan S, Herdman L, Alashi A, Centeno EH, Lyasheva M, Griffin BP, Flamm SD, Shirodaria C, Sabharwal N, Kelion A, Dweck MR, Van Beek EJR, Deanfield J, Hopewell JC, Neubauer S, Channon KM, Achenbach S, Newby DE, Antoniades C. A novel machine learning-derived radiotranscriptomic signature of perivascular fat improves cardiac risk prediction using coronary CT angiography. *Eur Heart J* 2019; **40**: 3529-3543 [PMID: 31504423 DOI: 10.1093/eurheartj/ehz592]

46   **Lin A**, Kolossváry M, Yuvaraj J, Cadet S, McElhinney PA, Jiang C, Nerlekar N, Nicholls SJ, Slomka PJ, Maurovich-Horvat P, Wong DTL, Dey D. Myocardial Infarction Associates With a Distinct Pericoronary Adipose Tissue Radiomic Phenotype: A Prospective Case-Control Study. *JACC Cardiovasc Imaging* 2020; **13**: 2371-2383 [PMID: 32861654 DOI: 10.1016/j.jcmg.2020.06.033]

47   **van Rosendael AR**, Maliakal G, Kolli KK, Beecy A, Al'Aref SJ, Dwivedi A, Singh G, Panday M, Kumar A, Ma X, Achenbach S, Al-Mallah MH, Andreini D, Bax JJ, Berman DS, Budoff MJ, Cademartiri F, Callister TQ, Chang HJ, Chinnaiyan K, Chow BJW, Cury RC, DeLago A, Feuchtner G, Hadamitzky M, Hausleiter J, Kaufmann PA, Kim YJ, Leipsic JA, Maffei E, Marques H, Pontone G, Raff GL, Rubinshtein R, Shaw LJ, Villines TC, Gransar H, Lu Y, Jones EC, Peña JM, Lin FY, Min JK. Maximization of the usage of coronary CTA derived plaque information using a machine learning based algorithm to improve risk stratification; insights from the CONFIRM registry. *J Cardiovasc Comput Tomogr* 2018; **12**: 204-209 [PMID: 29753765 DOI: 10.1016/j.jcct.2018.04.011]

48   **Motwani M**, Dey D, Berman DS, Germano G, Achenbach S, Al-Mallah MH, Andreini D, Budoff MJ, Cademartiri F, Callister TQ, Chang HJ, Chinnaiyan K, Chow BJ, Cury RC, Delago A, Gomez M, Gransar H, Hadamitzky M, Hausleiter J, Hindoyan N, Feuchtner G, Kaufmann PA, Kim YJ, Leipsic J, Lin FY, Maffei E, Marques H, Pontone G, Raff G, Rubinshtein R, Shaw LJ, Stehli J, Villines TC, Dunning A, Min JK, Slomka PJ. Machine learning for prediction of all-cause mortality in patients with suspected coronary artery disease: a 5-year multicentre prospective registry analysis. *Eur Heart J* 2017; **38**: 500-507 [PMID: 27252451 DOI: 10.1093/eurheartj/ehw188]

49   **Johnson KM**, Johnson HE, Zhao Y, Dowe DA, Staib LH. Scoring of Coronary Artery Disease Characteristics on Coronary CT Angiograms by Using Machine Learning. *Radiology* 2019; **292**: 354-362 [PMID: 31237495 DOI: 10.1148/radiol.2019182061]

50   **van Assen M**, Varga-Szemes A, Schoepf UJ, Duguay TM, Hudson HT, Egorova S, Johnson K, St Pierre S, Zaki B, Oudkerk M, Vliegenthart R, Buckler AJ. Automated plaque analysis for the prognostication of major adverse cardiac events. *Eur J Radiol* 2019; **116**: 76-83 [PMID: 31153577 DOI: 10.1016/j.ejrad.2019.04.013]

51   **von Knebel Doeberitz PL**, De Cecco CN, Schoepf UJ, Albrecht MH, van Assen M, De Santis D, Gaskins J, Martin S, Bauer MJ, Ebersberger U, Giovagnoli DA, Varga-Szemes A, Bayer RR 2nd, , Schönberg SO, Tesche C. Impact of Coronary Computerized Tomography Angiography-Derived Plaque Quantification and Machine-Learning Computerized Tomography Fractional Flow Reserve on Adverse Cardiac Outcome. *Am J Cardiol* 2019; **124**: 1340-1348 [PMID: 31481177 DOI: 10.1016/j.amjcard.2019.07.061]

52   **Commandeur F**, Slomka PJ, Goeller M, Chen X, Cadet S, Razipour A, McElhinney P, Gransar H, Cantu S, Miller RJH, Rozanski A, Achenbach S, Tamarappoo BK, Berman DS, Dey D. Machine learning to predict the long-term risk of myocardial infarction and cardiac death based on clinical risk, coronary calcium, and epicardial adipose tissue: a prospective study. *Cardiovasc Res* 2020; **116**: 2216-2225 [PMID: 31853543 DOI: 10.1093/cvr/cvz321]

53   **Kwan AC**, McElhinney PA, Tamarappoo BK, Cadet S, Hurtado C, Miller RJH, Han D, Otaki Y, Eisenberg E, Ebinger JE, Slomka PJ, Cheng VY, Berman DS, Dey D. Prediction of revascularization by coronary CT angiography using a machine learning ischemia risk score. *Eur Radiol* 2021; **31**: 1227-1235 [PMID: 32880697 DOI: 10.1007/s00330-020-07142-8]

Published by Baishideng Publishing Group Inc
7041 Koll Center Parkway, Suite 160, Pleasanton, CA 94566, USA
Telephone: +1-925-3991568
E-mail: bpgoffice@wjgnet.com
Help Desk: https://www.f6publishing.com/helpdesk
https://www.wjgnet.com